J Mater Sci (2006) 41:4901–4913
DOI 10.1007/s10853-006-0319-x

Elastic–plastic thermomechanical response of composite co-axial cylinders

L. H. You · Z. Y. Zheng

Received: 21 October 2002 / Accepted: 15 September 2005 / Published online: 27 May 2006

Abstract A new method is developed in this paper to deal with the thermomechanical response of continuous fiber-reinforced composites. Treating the matrix as an elastic-perfectly plastic solid, the analytical formulae of the deformations and stresses of the matrix are obtained from the plasticity theory, axisymmetric equilibrium equation, and stress–strain and strain–displacement relations. The fiber is taken to be an anisotropic, elastic material, and the formulae calculating its deformations and stresses are also presented. The boundary conditions and the consistence of deformations and stresses between the fiber and matrix, and between elastic and plastic regions of the matrix are employed to determine the unknown constants in the analytical formulae. With the developed method, the thermomechanical stress distributions in composites reinforced with circumferentially orthotropic, radially orthotropic and transversely isotropic fibers are investigated, and how the elastic-perfectly plastic property and different materials of the matrix affect the thermomechanical response of the composites is discussed. For the thermomechanical loads and composite systems given in this paper, the elastic-perfectly plastic property of the matrix can reduce the compressive stresses in the fiber, and the tensile circumferential and axial stresses in the matrix. A strong matrix can raise the compressive stresses in the fiber, and the tensile circumferential and axial stresses in the matrix.

L. H. You (✉)
College of Mechanical Engineering, Chongqing University, Chongqing City 400044, P.R. China
e-mail: lyou@bournemouth.ac.uk

L. H. You
NCCA, Bournemouth University, Poole BH12 5BB, UK

Z. Y. Zheng
School of Mechanical & Electrical Engineering, Chongqing Jiaotong University, Chongqing City 400074, P.R. China

Introduction

Due to different material properties of the constituents of the composites reinforced with continuous fibers, different deformations of the constituents will occur for the composites subjected to thermal or thermomechanical loads induced during processing or in-service exposure. They may cause large thermal or thermomechanical stresses and lead to composite failure or property degradation. Therefore, thermal or thermomechanical analysis of the composites has attracted a lot of attentions and some methods have been developed.

The concentric cylindrical model is the most popular one used in thermal and thermomechanical analyses of fibrous composites. Early in 1980, this model was employed to deal with the static problem of the linear theory of thermoelasticity for a composite cylinder by Iesan [1]. Using such a concentric cylinder model, Mikata and Taya investigated stress fields in a coated continuous fiber composite under thermomechanical loading [2]. Based on the Eshelby's method, Arsenault and Taya constructed a theoretical model to predict the thermal residual stresses in metal matrix composites [3]. Extending two- and four-concentric cylinder elastic models to a multi layer coaxial-cylinder elastic model, Warwick and Clyne carried out thermal stress analysis of SiC monofilament systems [4]. Using a three-phase cylinder model consisting of an inner fiber, middle interphase and outer matrix, Gardner

et al. examined how different Young's moduli of the interphase affect residual thermal stresses in filamentary polymer-matrix composites containing an elastomeric interphase [5, 6]. These research studies modeled the coating or interphase as a homogeneous region. However, the actual interphases may have spatial property variations. Using three different expressions to simulate the Young's modulus variations in the interphase and still taking the Poisson's ratio and thermal expansion coefficient to be constants, Jayaraman and Reifsnider discussed the effect of continuously varying Young's modulus in the fiber/matrix interphase on thermal residual stresses [7, 8]. Assuming the fibers to be arranged in a regular array in the matrix and employing the ADINA finite element package, Szyszkowski and King analyzed the thermal stress concentrations at the surface of the composites [9].

When the thermal deformations are large enough, one or more constituents of the composites may plastically yield. In order to tackle the plastic deformations of the composites under thermal or thermomechanical loads, the stress analysis of the composites subjected to thermal or thermomechanical loads was extended from full elasticity to plasticity. Based on von Mises' yield criterion, Zhang et al. developed an axisymmetric model for the thermally induced stresses and strains in a continuous fiber-reinforced composite with a plastic matrix and obtained two partial differential equations describing the deformations of the composites which must be solved iteratively [10]. Choo et al. presented a finite element analysis method to determine thermal residual stresses in continuous-fiber-reinforced composites [11]. Analytical expressions of deformations and stresses of the fibrous composites subjected to thermal or thermomechanical loads are simpler and more profound in the prediction of the thermal or thermomechanical response of the composites. An analytical method was developed by You et al. to cope with the plastic deformations of coating and matrix [12, 13].

The above work treated the constituent materials of the composites as fully elastic or elastic–plastic with a strain–hardening behaviour. However, many materials, having been used as some constituents of the composites, exhibit an elastic-perfectly plastic behaviour. For the composites containing such constituent materials, new approaches must be developed to perform their stress analysis. In this paper, the matrix of the composites is treated as an isotropic, elastic-perfectly plastic solid. Tresca's yield criterion in plasticity is employed to derive the deformations and stresses of the matrix. The fiber is taken as an anisotropic, elastic solid. The analytical formulae of its thermomechanical deformations and stresses are obtained from the theory of anisotropic elasticity. The resolution equations of the composites consisting of such a matrix and fiber are derived from the boundary conditions, the consistence of deformations and stresses at the interfaces between the fiber and matrix, and between elastic and plastic regions of the matrix. By solving these equations, all unknown constants in the analytical formulae are determined. Using the developed method, we investigate the stresses in the composites reinforced with circumferentially orthotropic, radially orthotropic and transversely isotropic fibers subjected to axisymmetric thermomechanical loads and discuss how different matrices affect the thermomechanical response of the composites.

Analytical formulae of deformations and stresses

The composites to be studied consist of continuous anisotropic fibers and an elastic-perfectly plastic matrix. Subject to axisymmetric thermomechanical loads, the composites can be simplified as a two-phase concentric cylinder model as shown in Fig. 1 where r_f and r_m represent the outer radii of the fiber and matrix, respectively.

When the deformation of the matrix is big enough, it may become plastic yield. In the theory of plasticity, there are usually two plastic yield criteria: Tresca's yield criterion and von Mises' yield criterion. In order to reach an analytical mathematical expression of deformations and stresses of the composites subject to axisymmetric thermomechanical loading, we here employ Tresca's yield criterion to derive the governing equation. When using Tresca's yield criterion, the maximum and minimum normal stresses must be known. It is often impossible before we obtain the stress distribution in the composites. However, since three normal stress components only have six different combinations, we can use Tresca's yield criterion to derive the governing equations

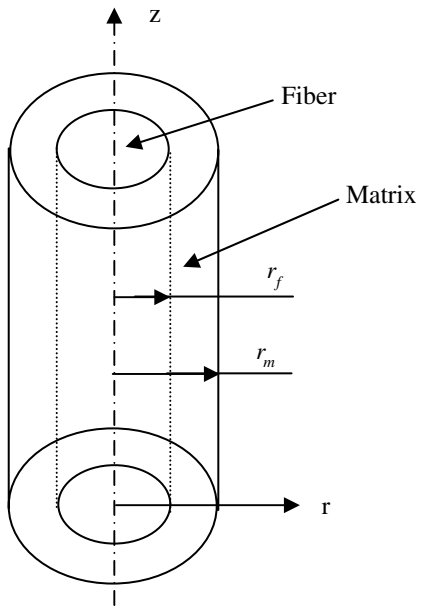

Fig. 1 The concentric cylinder model of continuous fiber-reinforced composites

for all the stress combinations. For example, we assume that the circumferential stress is the largest and the radial stress is the smallest. Tresca's yield criterion for this stress combination can be written as

$$\sigma_\theta - \sigma_r = \sigma_y \tag{1}$$

where σ_θ, σ_r and σ_y are the circumferential, radial and yield stresses of the matrix, respectively.

Under axisymmetric thermomechanical loads, the deformations and stresses in the composite model are axisymmetric. Without considering the effect of shear stresses, the stress equilibrium equations for this case have the forms of

$$\begin{aligned} r\frac{\mathrm{d}\sigma_r}{\mathrm{d}r} + \sigma_r - \sigma_\theta &= 0 \\ \frac{\mathrm{d}\sigma_z}{\mathrm{d}z} &= 0 \end{aligned} \tag{2}$$

where σ_z is the axial stress, and r is the radial coordinate.

The second of Eq. 2 gives

$$\sigma_z = c_1 \tag{3}$$

where c_1 is an unknown constant.

Substituting Eq. 1 into the first of Eq. 2, we obtain a first order ordinary differential equation, its resolution gives the radial stress as follows

$$\sigma_r = \sigma_y \ln r + c_2 \tag{4}$$

where c_2 is an unknown constant.

The substitution of the radial stress (4) into Tresca's yield criterion (1) gives the following circumferential stress

$$\sigma_\theta = \sigma_y(1 + \ln r) + c_2 \tag{5}$$

For an isotropic, elastic solid, the relationships between the strains and stresses can be described with Hooke's law which have the forms of

$$\begin{aligned} \varepsilon_r^e &= \frac{1}{E}[\sigma_r - v(\sigma_\theta + \sigma_z)] \\ \varepsilon_\theta^e &= \frac{1}{E}[\sigma_\theta - v(\sigma_r + \sigma_z)] \\ \varepsilon_z^e &= \frac{1}{E}[\sigma_z - v(\sigma_\theta + \sigma_r)] \end{aligned} \tag{6}$$

where E is Young's modulus, v is Poisson's ratio, and ε_r^e, ε_θ^e and ε_z^e are radial, circumferential and axial elastic strains, respectively.

Subjected to axisymmetric thermomechanical loads, the total deformations of the matrix after yielding can be divided into elastic, plastic and thermal ones, i.e.,

$$\begin{aligned} \varepsilon_r &= \varepsilon_r^e + \varepsilon_r^p + \varepsilon_r^t \\ \varepsilon_\theta &= \varepsilon_\theta^e + \varepsilon_\theta^p + \varepsilon_\theta^t \\ \varepsilon_z &= \varepsilon_z^e + \varepsilon_z^p + \varepsilon_z^t \end{aligned} \tag{7}$$

where the superscripts e, p and t represent the elastic, plastic and thermal strains, respectively.

According to Eq. 1, Tresca's yield function f is

$$f = \sigma_\theta - \sigma_r - \sigma_y \tag{8}$$

From the plastic potential theory [14], the relations among the plastic stain components can be derived from Eq. 8 and can be written as

$$\begin{aligned} \varepsilon_r^p &= -\varepsilon_\theta^p \\ \varepsilon_z^p &= 0 \end{aligned} \tag{9}$$

For an isotropic solid, the thermal expansion coefficient along the three orthogonal directions is the same and the thermal strains can be determined with the formula

$$\varepsilon_r^t = \varepsilon_\theta^t = \varepsilon_z^t = \alpha\Delta T \tag{10}$$

where α is the thermal expansion coefficient of the matrix, and ΔT is a uniform temperature change.

Substituting Eqs. 6, 9 and 10 into 7, then superimposing the total radial, circumferential and axial strains, the following relation is obtained

$$\varepsilon_r + \varepsilon_\theta + \varepsilon_z = \frac{1-2v}{E}(\sigma_r + \sigma_\theta + \sigma_z) + 3\alpha\Delta T \tag{11}$$

For axisymmetric deformations, the strain components are related to the displacement components with the following equations

$$\begin{aligned} \varepsilon_r &= \frac{\mathrm{d}u}{\mathrm{d}r} \\ \varepsilon_\theta &= \frac{u}{r} \\ \varepsilon_z &= \frac{\mathrm{d}w}{\mathrm{d}z} \end{aligned} \tag{12}$$

where u and w are the radial and axial displacements, respectively.

Substituting the axial stress (3), radial stress (4) and circumferential stress (5) into the third of Eq. 6, the elastic axial strain is obtained. Substituting the elastic axial strain, the second of Eq. 9 and the thermal strain (10) into the third of Eq. 7, we obtain the total axial strain ε_z. Substituting the total axial strain ε_z into the third of Eq. 12 and integrating, the axial displacement is found to be

$$w = \frac{1}{E}\left[c_1 - v\sigma_y(1 + 2\ln r) - 2vc_2\right]z + \alpha\Delta T z + c_3 \tag{13}$$

where c_3 is an unknown constant.

Substituting the stress components (3), (4) and (5) into Eq. 11 and making use of the relationships (12) between the strains and displacements, the following first order ordinary differential equation is obtained

$$\frac{\mathrm{d}u}{\mathrm{d}r} + \frac{u}{r} = \frac{1-v}{E}\left[\sigma_y(1 + 2\ln r) - \frac{2v}{1-v}c_1 + 2c_2\right] + 2\alpha\Delta T \tag{14}$$

By solving the above equation, the radial displacement is determined as follows

$$u = \frac{1-v}{E}\left(-\frac{v}{1-v}c_1 + c_2 + \sigma_y \ln r\right)r + c_4 r^{-1} + \alpha\Delta T r \tag{15}$$

where c_4 is an unknown constant.

For the elastic deformation of the matrix, the radial and axial displacements, and the radial, circumferential and axial stresses can be derived from the relationships between strains and displacements (12) and between strains and stresses (6) together with the equilibrium Eq. 2. They have the forms of [15]

$$u = c_6 r + c_7 r^{-1} \tag{16}$$

$$w = \frac{1}{1-v}\left[\frac{1-v-2v^2}{E}c_5 - 2vc_6 + (1+v)\alpha\Delta T\right]z + c_8 \tag{17}$$

$$\begin{aligned}
\sigma_r &= \frac{v}{1-v}c_5 + \frac{E}{1-v}c_6 - \frac{E}{1+v}c_7 r^{-2} - \frac{E}{1-v}\alpha\Delta T \\
\sigma_\theta &= \frac{v}{1-v}c_5 + \frac{E}{1-v}c_6 + \frac{E}{1+v}c_7 r^{-2} - \frac{E}{1-v}\alpha\Delta T \\
\sigma_z &= c_5
\end{aligned} \tag{18}$$

where c_5, c_6, c_7 and c_8 are the unknown constants.

For the elastic deformations of anisotropic fibers whose material property symmetry has two orthogonal planes, the equilibrium Eq. 2 and geometric Eq. 12 keep unchanged. However, the stress–strain relation (6) must be replaced with the following equations [16]

$$\begin{aligned}
\sigma_r &= c_{rr}(\varepsilon_r - \alpha_r\Delta T) + c_{r\theta}(\varepsilon_\theta - \alpha_\theta\Delta T) + c_{rz}(\varepsilon_z - \alpha_z\Delta T) \\
\sigma_\theta &= c_{\theta r}(\varepsilon_r - \alpha_r\Delta T) + c_{\theta\theta}(\varepsilon_\theta - \alpha_\theta\Delta T) + c_{\theta z}(\varepsilon_z - \alpha_z\Delta T) \\
\sigma_z &= c_{zr}(\varepsilon_r - \alpha_r\Delta T) + c_{z\theta}(\varepsilon_\theta - \alpha_\theta\Delta T) + c_{zz}(\varepsilon_z - \alpha_z\Delta T)
\end{aligned} \tag{19}$$

where $c_{ij}(i, j{=}\theta, r, z)$ represent the stiffness coefficients, and α_r, α_θ and α_z are the thermal expansion coefficients of the fiber along radial, circumferential and axial directions, respectively.

The radial and axial displacements and radial, circumferential and axial stresses in the fiber can also be obtained from Eqs. 2, 12 and 19 which can be written as [17, 18]

$$u = c_9 A r + c_{10} r^{\lambda_{f1}} + c_{11} r^{\lambda_{f2}} + Br \tag{20}$$

$$\begin{aligned}
w = \Bigg[&\frac{1 - A(c_{z\theta} + c_{zr})}{c_{zz}}c_9 - \frac{B(c_{z\theta} + c_{zr})}{c_{zz}} \\
&- \frac{c_{10}}{c_{zz}}(c_{z\theta} + \lambda_{f1}c_{zr})r^{\lambda_{f1}-1} - \frac{c_{11}}{c_{zz}}(c_{z\theta} + \lambda_{f2}c_{zr})r^{\lambda_{f2}-1} \\
&+ \frac{1}{c_{zz}}(c_{z\theta}\alpha_\theta + c_{zr}\alpha_r + c_{zz}\alpha_z)\Delta T\Bigg]z + c_{12}
\end{aligned} \tag{21}$$

$$\begin{aligned}
\sigma_r =& c_9\left\{\frac{c_{rz}}{c_{zz}} + A\left[c_{r\theta} + c_{rr} - \frac{c_{rz}}{c_{zz}}(c_{z\theta} + c_{zr})\right]\right\} + c_{10}[c_{r\theta} \\
&+ \lambda_{f1}c_{rr} - \frac{c_{rz}}{c_{zz}}(c_{z\theta} + \lambda_{f1}c_{zr})]r^{\lambda_{f1}-1} \\
&+ c_{11}[c_{r\theta} + \lambda_{f2}c_{rr} - \frac{c_{rz}}{c_{zz}}(c_{z\theta} + \lambda_{f2}c_{zr})]r^{\lambda_{f2}-1} \\
&+ B\left[c_{r\theta} + c_{rr} - \frac{c_{rz}}{c_{zz}}(c_{z\theta} + c_{zr})\right] + \\
&\left[\frac{c_{rz}}{c_{zz}}(c_{z\theta}\alpha_\theta + c_{zr}\alpha_r) - (c_{r\theta}\alpha_\theta + c_{rr}\alpha_r)\right]\Delta T \\
\sigma_\theta =& c_9\left\{\frac{c_{\theta z}}{c_{zz}} + A\left[c_{\theta\theta} + c_{\theta r} - \frac{c_{z\theta}}{c_{zz}}(c_{\theta z} + c_{zr})\right]\right\} \\
&+ c_{10}[c_{\theta\theta} + \lambda_{f1}c_{\theta r} - \frac{c_{z\theta}}{c_{zz}}(c_{\theta z} + \lambda_{f1}c_{zr})]r^{\lambda_{f1}-1} \\
&+ c_{11}[c_{\theta\theta} + \lambda_{f2}c_{\theta r} - \frac{c_{z\theta}}{c_{zz}}(c_{\theta z} + \lambda_{f2}c_{zr})]r^{\lambda_{f2}-1} \\
&+ B\left[c_{\theta\theta} + c_{\theta r} - \frac{c_{z\theta}}{c_{zz}}(c_{\theta z} + c_{zr})\right] \\
&+ \left[\frac{c_{\theta z}}{c_{zz}}(c_{z\theta}\alpha_\theta + c_{zr}\alpha_r) - (c_{\theta\theta}\alpha_\theta \right. \\
&\left. + c_{\theta r}\alpha_r)\right]\Delta T \\
\sigma_z =& c_9
\end{aligned} \tag{22}$$

where

and c_9, c_{10}, c_{11} and c_{12} are unknown constants.

$$\lambda_{f1,f2} = \pm\sqrt{\frac{c_{zz}c_{\theta\theta} - c_{z\theta}c_{\theta z}}{c_{zz}c_{rr} - c_{zr}c_{rz}}}$$
$$A = \frac{c_{rz} - c_{\theta z}}{c_{zz}c_{\theta\theta} + c_{zr}c_{rz} - c_{zz}c_{rr} - c_{z\theta}c_{\theta z}} \tag{23}$$
$$B = \frac{[(c_{zz}c_{\theta\theta} + c_{z\theta}c_{rz} - c_{zz}c_{r\theta} - c_{z\theta}c_{\theta z})\alpha_\theta + (c_{zz}c_{\theta r} + c_{zr}c_{rz} - c_{zz}c_{rr} - c_{\theta z}c_{zr})\alpha_r]\Delta T}{c_{zz}c_{\theta\theta} + c_{zr}c_{rz} - c_{zz}c_{rr} - c_{z\theta}c_{\theta z}}$$

For the perfect bonding at the interface between the fiber and matrix, the deformations of the fiber and matrix at this interface must be the same. The radial stresses of the fiber and matrix at this interface must keep continuous. In addition, the deformations and stresses at the interface between the elastic and plastic regions of the matrix must be the same as well. Taking the axisymmetric mechanical loads to be an externally applied radial stress σ_{r0} and an externally applied axial stress σ_{z0}, these conditions of deformations and stresses together with the boundary conditions of the composites can be written as

$$\begin{aligned}
&u_f \text{ is a bounded value} && \text{at } r = 0\\
&w_{zf} = w^p_{zm} = w^e_{zm} = 0 && \text{at z} = 0\\
&u_f = u^p_m \quad w_{zf} = w^p_{zm} \quad \sigma_{rf} = \sigma^p_{rm} && \text{at } r = r_f\\
&u^p_m = u^e_m \quad w^p_{zm} = w^e_{zm} \quad \sigma^p_{rm} = \sigma^e_{rm} \quad \sigma^p_{\theta m} = \sigma^e_{\theta m} && \text{at } r = r_\xi\\
&\sigma^e_{rm} = \sigma_{r0} && \text{at } r = r_m\\
&\int_0^{r_f} \sigma_{zf} r\mathrm{d}r + \int_{r_f}^{r_\xi} \sigma^p_{zm} r\mathrm{d}r + \int_{r_\xi}^{r_m} \sigma^e_{zm} r\mathrm{d}r = \int_0^{r_m} \sigma_{z0} r\mathrm{d}r
\end{aligned} \tag{24}$$

where r_ξ is the interface radius between the elastic and plastic regions of the matrix, the superscripts e and p represent elastic and plastic regions, the subscripts f and m stand for the fiber and matrix, and the subscripts r, θ and z indicate the radial, circumferential and axial directions, respectively.

Substituting the radial and axial displacements, and radial, circumferential and axial stresses of the fiber and matrix into Eq. 24, we obtain 13 linear algebra equations. Their resolution determines 13 unknown constants c_1–c_{12} and the interface radius r_ξ between the elastic and plastic regions of the matrix.

Numerical applications

Using the above-developed analytical method, in this section, we investigate the thermomechanical stresses in the composites comprising an anisotropic fiber and elastic-perfectly plastic matrix. Three types of anisotropic fibers are taken into account. They are radially orthotropic fibers, circumferentially orthotropic fibers and transversely isotropic fibers. The material properties of the fibers and matrices are listed in Table 1 where ROF, COF and TIF represent a radially orthotropic fiber, a circumferentially orthotropic fiber and a transversely isotropic fiber, respectively. The material properties of Matrix 1 are from those of Ti-24Al-11Nb and its yield stress is σ_y = 371.5 *MPa* [19]. The material properties of Matrix 2 are based on those of polycrystalline NiAl and its yield stress is σ_y = 1453 *MPa* [11].

The outer radius of the fiber is taken to be 40 μm and that of the matrix is 70 μm. A uniform temperature decrease of –800°C, an externally applied radial stress of 150 MPa and axial stress of –300 MPa are applied on the composites. Firstly, we consider Matrix 1 in Table 1. The obtained non-dimensional radial, circumferential and axial stresses in the fiber are depicted in Figs. 2–4, and those in matrix in Figs. 5–7. The non-dimensional Tresca's equivalent stresses in the matrix are given in Fig. 8. In the figures, σ_{y1} is the yield stress of Matrix 1, the uppercase letter *P* means the non-dimensional stresses are from an elastic-perfectly plastic matrix, and the uppercase letter *E* indicates the non-dimensional stresses are from a fully elastic matrix. For instance, COFP represents the non-dimensional stresses in the composites comprising a circumferentially orthotropic fiber and an elastic-perfectly

Table 1 Material properties of fibers and matrices

	E_z (GPa)	E_θ (GPa)	E_r (GPa)	$\nu_{z\theta}$	ν_{zr}	$\nu_{\theta r}$	$\alpha_z(10^{-6}/°C)$	$\alpha_\theta(10^{-6}/°C)$	$\alpha_r(10^{-6}/°C)$
ROF	480	250	480	0.19	0.25	0.19	2.5	3.3	2.5
COF	480	480	250	0.19	0.25	0.25	2.5	2.5	3.3
TIF	480	250	250	0.19	0.19	0.25	2.5	3.3	3.3
Matrix 1	110.3	110.3	110.3	0.26	0.26	0.26	9	9	9
Matrix 2	167.3	167.3	167.3	0.3	0.3	0.3	13.05	13.05	13.05

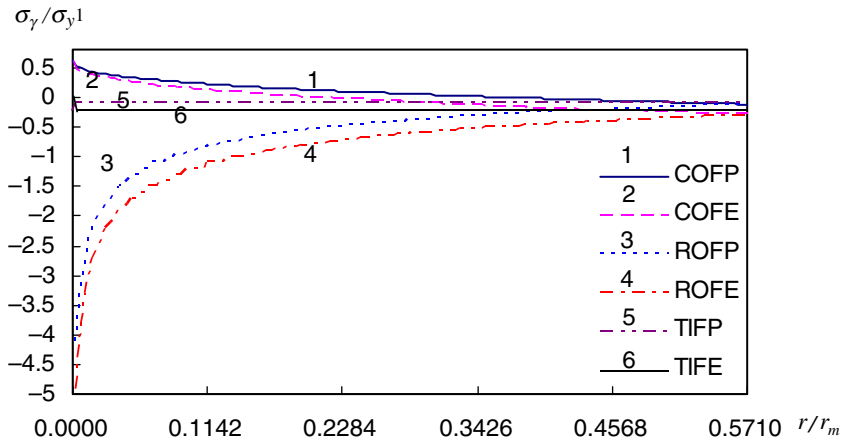

Fig. 2 Radial stresses in fiber of composites (Matrix 1)

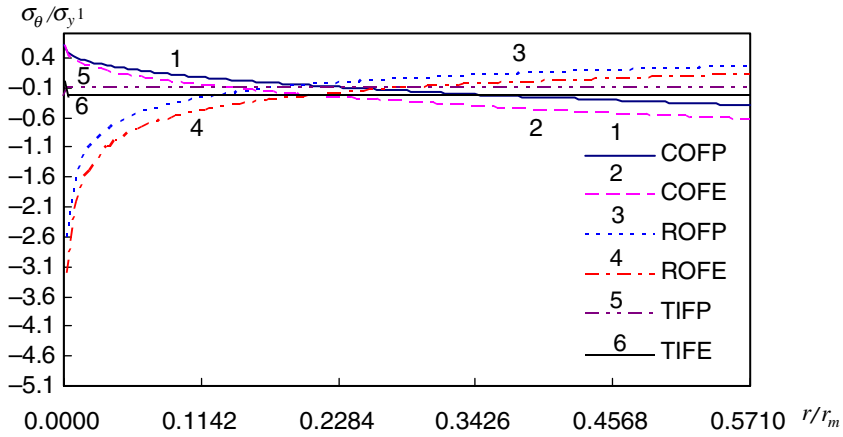

Fig. 3 Circumferential stresses in fiber of composites (Matrix 1)

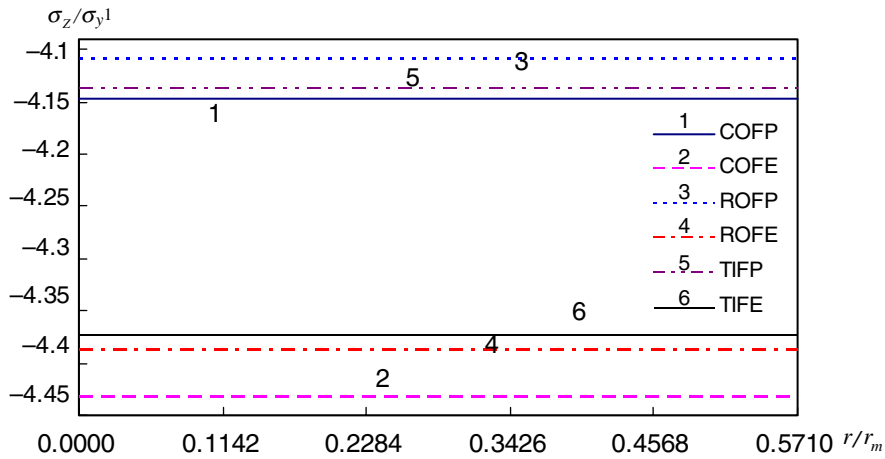

Fig. 4 Axial stresses in fiber of composites (Matrix 1)

plastic matrix, and ROFE stands for those in the composites containing a radially orthotropic fiber and a fully elastic matrix.

Figure 2 indicates that the compressive radial stresses in the fiber for the composites reinforced with the three types of fibers are decreased and the tensile radial stresses are increased after considering the elastic-perfectly plastic property of the matrix. Among them, the decrease of the radial stresses in the fiber for the composites reinforced with a radially orthotropic fiber is the largest. For different types of fibers, the radial stress distributions are different. For the composites reinforced with a transversely isotropic fiber, the radial stresses in the fiber keep unchanged along the radial direction. However, they exhibit quite different

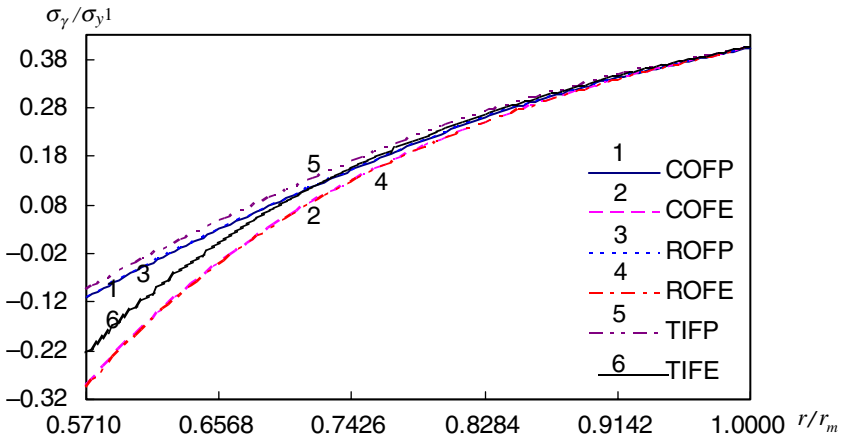

Fig. 5 Radial stresses in matrix of composites (Matrix 1)

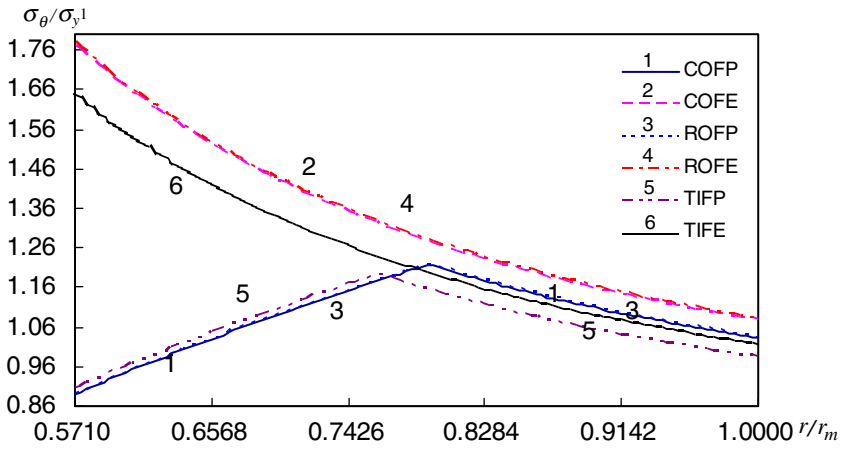

Fig. 6 Circumferential stresses in matrix of composites (Matrix 1)

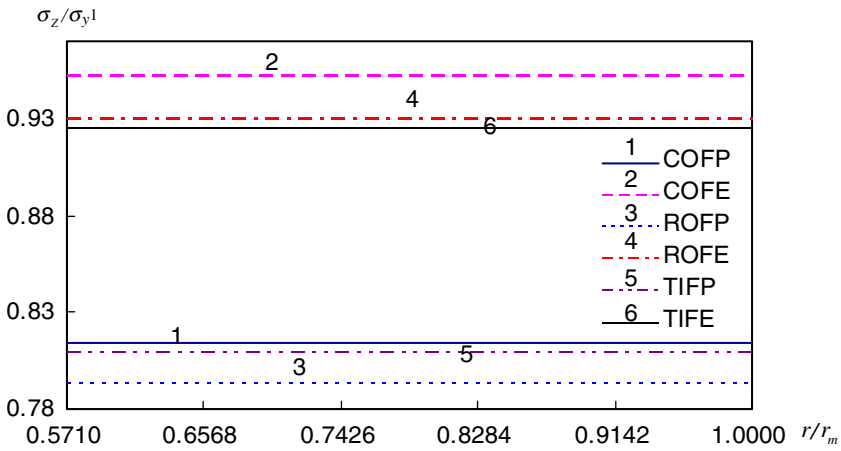

Fig. 7 Axial stresses in matrix of composites (Matrix 1)

distributions for the composites reinforced with other two types of fibers. For the composites reinforced with a circumferentially orthotropic fiber, the radial stresses in the region around the axis of the fiber are tensile. They drop when moving away from the axis of the fiber, and become compressive. For the composites reinforced with a radially orthotropic fiber, the radial stresses in the fiber are compressive. When moving towards the axis of the fiber, the compressive radial stresses rise. Especially in the region close to the axis of the fiber, the compressive radial stresses go up very fast. The circumferential stress distributions in the fiber are similar to those of the radial stresses (Fig. 3).

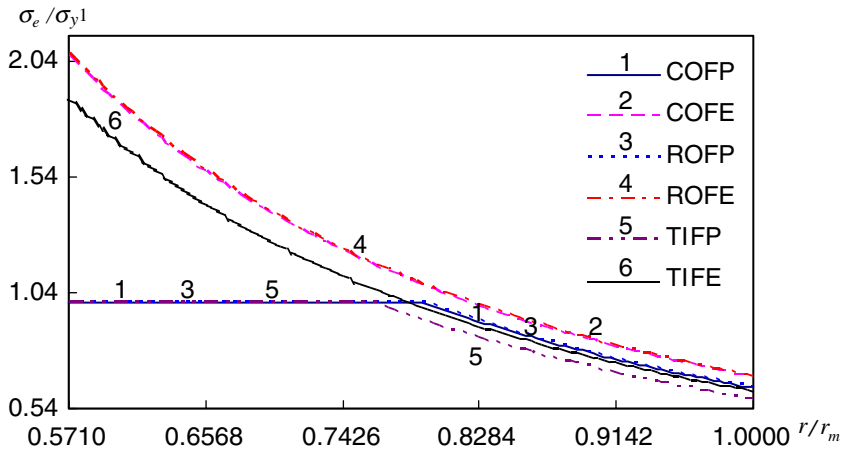

Fig. 8 Tresca's equivalent stresses in matrix of composites (Matrix 1)

For the composites reinforced with a transversely isotropic fiber, the circumferential stresses in the fiber are almost the same as the radial stresses. For the composites reinforced with a circumferentially orthotropic fiber, the radial and circumferential stresses in a very small region around the axis of the fiber are also almost the same. However, accompanying the increase of the radial coordinate, the circumferential stresses drop more quickly than the radial stresses. For the composites reinforced with a radially orthotropic fiber, the circumferential stresses in the fiber are much smaller than the radial stresses in the region very close to the axis of the fiber. The axial stresses in the fiber for the composites reinforced with the three types of fibers are always independent of the radial coordinate (Fig. 4). After the matrix partially yields, its restraint on the deformation of the fiber is weakened leading to smaller compressive axial stresses than those from the fully elastic matrix. The decreases of the axial stresses for the composites reinforced with circumferentially and radially orthotropic fibers are basically the same which are bigger than the reduction of the axial stresses in the fiber for the composites reinforced with a transversely isotropic fiber.

The compressive radial stresses in the matrix for the composites reinforced with circumferentially and radially orthotropic fibers are almost the same which are bigger than those for the composites reinforced with a transversely isotropic fiber (Fig. 5). All the radial stresses gradually change from the compressive ones at the interface between the fiber and matrix to the externally applied tensile radial stress at the outer radius of the matrix. After taking into account the elastic-perfectly plastic property of the matrix, the compressive radial stresses are decreased and the tensile radial stresses are increased obviously. The differences between the fully elastic and elastic-perfectly plastic ones become smaller and smaller along with the increase of the radial coordinate and disappear at the outer radius of the matrix. Without considering the elastic-perfectly plastic property of the matrix, the circumferential stresses for composites reinforced with circumferentially and radially orthotropic fibers are also very close and bigger than the circumferential stress in the composites reinforced with a transversely isotropic fiber (Fig. 6). All the circumferential stresses are the largest at the inner radius of the matrix. Then they drop along with the increase of the radial coordinate and reach their minimum values at the outer radius of the matrix. After taking into account the effect of the elastic-perfectly plastic property of the matrix, the circumferential stress distributions in the matrix are totally changed. At first, they go up from their minimum values at the inner radius of the matrix and reach their maximum values in some radial positions in the matrix. Then they go down until reaching the outer radius of the matrix. Such a variety of the circumferential stresses can be explained with Tresca's yield criterion. For the composites subjected to the above temperature change and externally applied radial and axial loads, the circumferential stress in the matrix is the largest and radial stress is the smallest. Therefore, Tresca's yield criterion for this stress state is $\sigma_\theta - \sigma_r = \sigma_y$. At the inner radius of the matrix, the radial stresses are compressive and the largest for the composites reinforced with the three types of fibers. Since the yield stress σ_y of the matrix is a constant, in order to satisfy the Tresca's yield criterion, the circumferential stresses must be the smallest. As the radial coordinate increases, the compressive radial stresses drop. Accordingly, the circumferential stresses increase. At the interfaces between the elastic and plastic regions of the matrix, the circumferential stresses reach their maximum values. Then, they decrease until reaching the outer radius of the matrix. Since Young's modulus of the matrix is far lower than Young' moduli of the fiber, the tensile axial stresses in the matrix are much smaller than the compressive axial stresses in the fiber. Like the axial stresses in the fiber, the axial stresses in the matrix are also independent of the radial coordinate (Fig. 7). After incorporating the elastic-perfectly plastic property of the matrix, the tensile axial stresses in the

matrix are also greatly lowered. Once again, the decreases of the axial stresses in the matrix for the composites reinforced with circumferentially and radially orthotropic fibers are almost the same and bigger than the reduction of the axial stresses for the composites reinforced with a transversely isotropic fiber.

Figure 8 gives the varieties of non-dimensional Tresca's equivalent stresses $\sigma_e/\sigma_{y1}=(\sigma_{max}-\sigma_{min})/\sigma_{y1}$ in the matrix. When the matrix is fully elastic, Tresca's equivalent stresses are the largest at the inner radius of the matrix for the composites reinforced with the three types of fibers. As the radial coordinate rises, they drop and reach their minimum values at the outer radius of the matrix. Also, Tresca's equivalent stresses for the composites reinforced with circumferentially and radially orthotropic fibers are basically identical and larger than Tresca's equivalent stress for the composites reinforced with a transversely isotropic fiber. After considering the elastic-perfectly plastic property of the matrix, the yielding firstly occurs at the inner radius of the matrix and Tresca's equivalent stresses are equal to the yield stress of the matrix. After that, Tresca's equivalent stresses keep unchanged until the difference between the maximum and minimum stresses is less than the yield stress of the matrix. Therefore, in the plastic region of the matrix, Tresca's equivalent stresses for the composites reinforced with the three types of fibers are the same and independent of the radial coordinate as demonstrated in Fig. 8. However, after moving into the elastic region of the matrix, only Tresca's equivalent stresses for the composites reinforced with circumferentially and radially orthotropic fibers are almost the same. Tresca's equivalent stress for the composites reinforced with a transversely isotropic fiber is changed to a smaller value. Then, all of them decrease along the radial direction and reach their minimum values at the outer radius of the matrix.

In the following, we examine how different matrix materials affect the thermomechanical response of the composites reinforced with anisotropic fibers. For doing this, we change the matrix material from Matrix 1 to Matrix 2 in Table 1 and still keep the fiber material unchanged. Since Young's modulus and yield stress of Matrix 2 are far higher than those of Matrix 1, Matrix 2 is stronger than Matrix 1. Using the same thermomechanical loads, the obtained non-dimensional radial, circumferential and axial stresses in the fiber are given in Figs. 9–11, those in the matrix in Figs. 12–14, and non-dimensional Tresca's equivalent stresses in the matrix are shown in Fig. 15. In all the figures, the capital letter *W* indicates the composites contain the weaker matrix, i. e., Matrix 1 and *S* means the composites comprise the stronger matrix, i. e., Matrix 2. For example, *ROFPW* represents the non-dimensional elastic–plastic stresses in the composites comprising a radially orthotropic fiber and the weaker matrix. And *TIFPS* stands for those in the composites containing a transversely isotropic fiber and the stronger matrix.

From the stress distributions in the fibers given by Figs. 9–11, it is clear that the stronger Matrix 2 greatly raises all the compressive stresses in the fibers. The radial stress in the fiber for the composites reinforced with a circumferentially orthotropic fiber is still tensile within a very small region around the axis of the fiber (Fig. 9). Then, it becomes compressive and increases more quickly than that caused by Matrix 1 when moving away from the axis of the fiber. At the outer radius of the fiber, the compressive radial stress reaches its maximum value. For the composites reinforced with a transversely isotropic fiber, the compressive radial stress in the fiber caused by Matrix 2 also keeps constant. However, it is much bigger than that caused by Matrix 1. The most obvious change is from the composites reinforced with a radially orthotropic fiber. For such composites, the difference of the radial

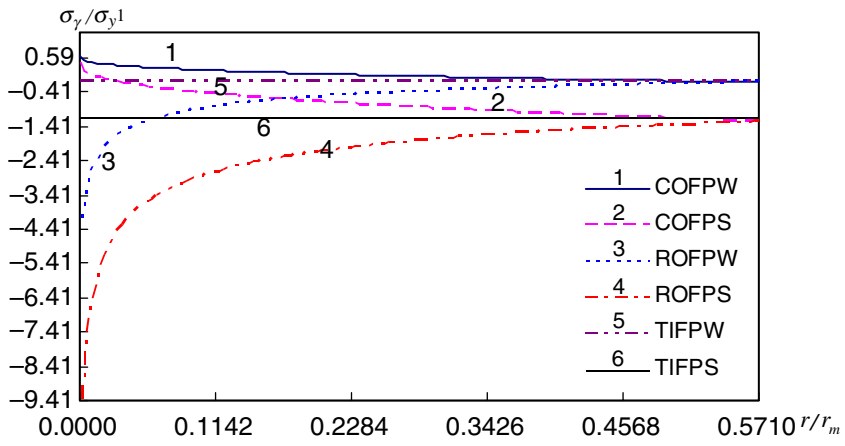

Fig. 9 Radial stresses in fiber of composites (Matrix 1 and Matrix 2)

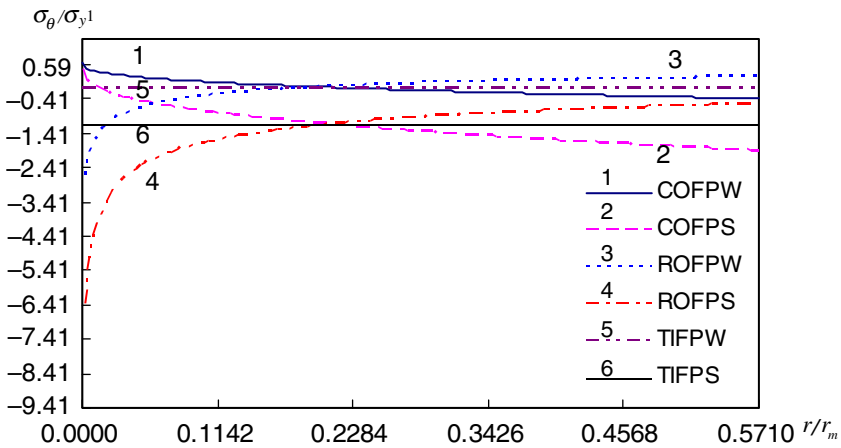

Fig. 10 Circumferential stresses in fiber of composites (Matrix 1 and Matrix 2)

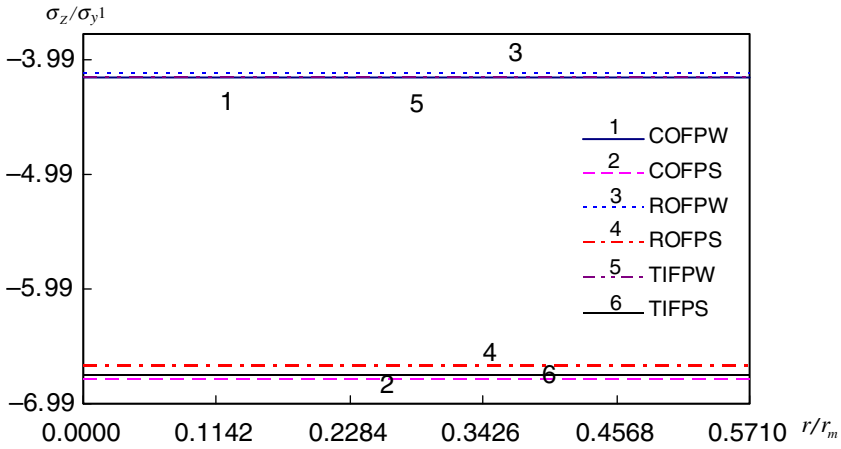

Fig. 11 Axial stresses in fiber of composites (Matrix 1 and Matrix 2)

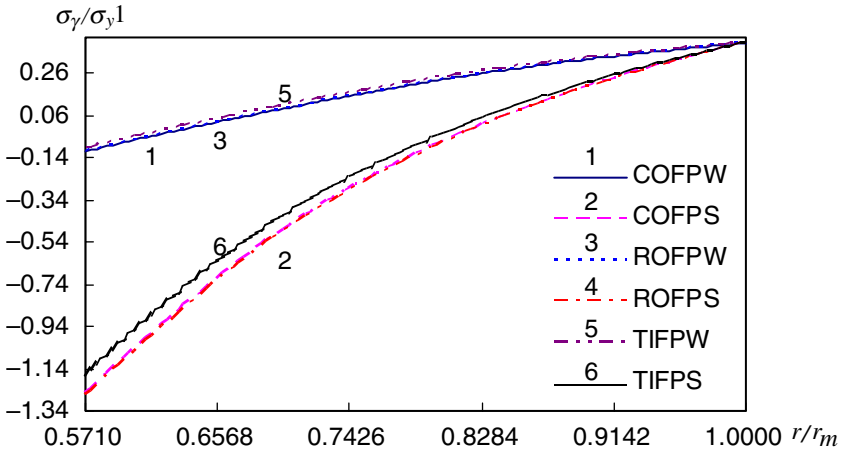

Fig. 12 Radial stresses in matrix of composites (Matrix 1 and Matrix 2)

stresses caused by Matrix 2 and Matrix 1 is the largest among all the composites. When moving towards the axis of the fiber, the radial stresses become bigger and bigger. At the position very close to the axis of the fiber, the radial stress caused by the stronger matrix is about 240% of that caused by the weaker matrix. The circumferential stress distributions in the fiber for the composites reinforced with the three types of fibers are similar to the radial stress distributions (Fig. 10). For the composites reinforced with a circumferentially orthotropic fiber, the difference of the circumferential stresses caused by the stronger matrix and weaker matrix becomes larger and larger relative to that of

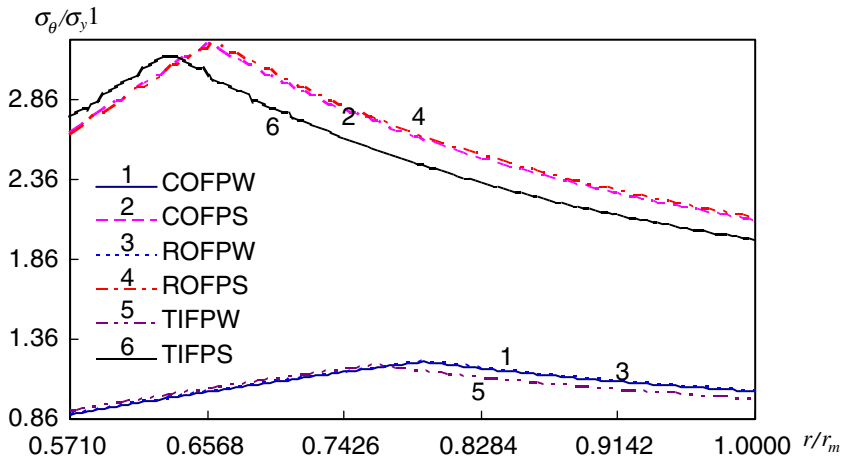

Fig. 13 Circumferential stresses in matrix of composites (Matrix 1 and Matrix 2)

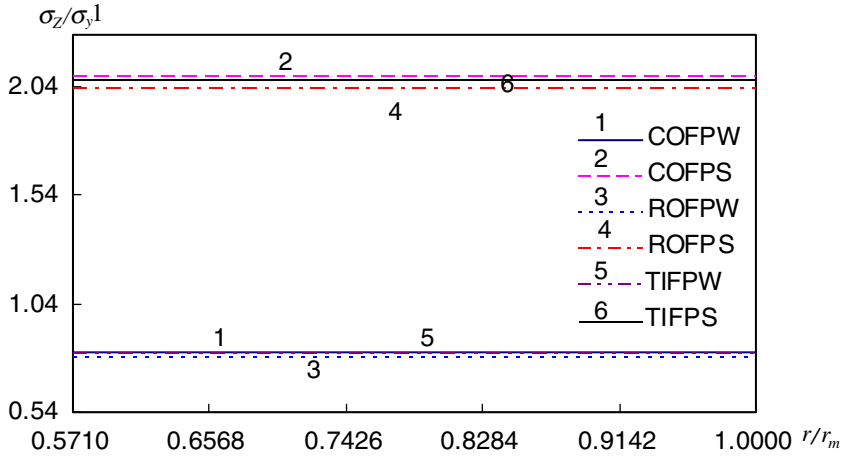

Fig. 14 Axial stresses in matrix of composites (Matrix 1 and Matrix 2)

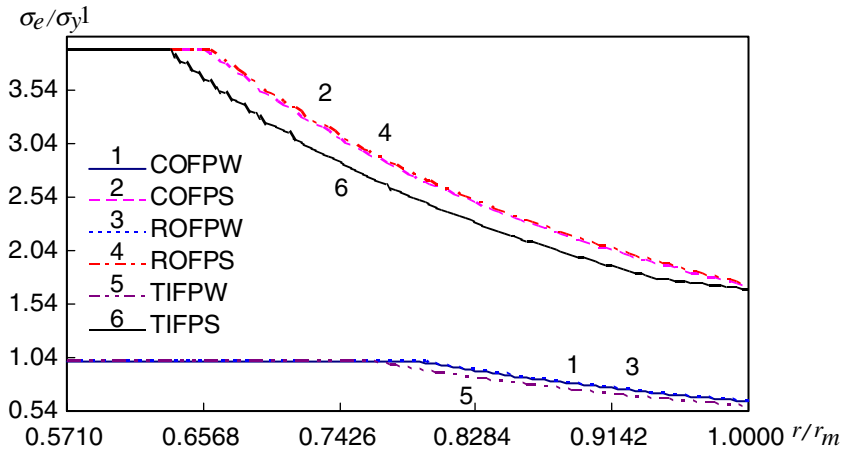

Fig. 15 Tresca's equivalent stresses in matrix of composites (Matrix 1 and Matrix 2)

the radial stresses when moving towards the outer radius of the fiber. Oppositely, this difference for the composites reinforced with a radially orthotropic fiber becomes smaller and smaller. At the same position very close to the axis of the fiber, the circumferential stress caused by the stronger matrix is still about 240% of that caused by the weaker matrix. Different from the above two cases, the differences of radial and circumferential stresses caused by the two different matrices are basically the same for the composites reinforced with a transversely isotropic fiber. The changes of the compressive axial stresses in the fiber for the composites reinforced with the three types of fibers are similar

after using the stronger matrix (Fig. 11). Compared to those from the weaker matrix, the compressive axial stresses in the fiber from the stronger matrix are increased by about 60% for the composites reinforced with the three types of fibers.

The obvious increase of all the compressive stresses in the fiber can be explained with the material properties of the matrix. Firstly, the thermal expansion coefficients of Matrix 2 and Matrix 1 are 13.05×10^{-6}/°C and 9×10^{-6}/°C, respectively. Therefore, thermal deformation difference between the fiber and matrix caused by the stronger matrix is bigger than that caused by the weaker matrix. Next, Young's moduli of Matrix 2 and Matrix 1 are 167.3 GPa and 110.3 GPa, respectively. The higher Young's modulus applies a stronger restraint on the deformation of the fiber leading to higher compressive stresses in the fiber. Finally, the yield stress of the stronger matrix is much bigger than that of the weaker matrix. Therefore, the plastic deformation of the stronger matrix is more difficult to occur than the weaker matrix resulting in larger compressive stresses in the fiber.

Similar to the increase of the compressive radial stresses in the fiber, the compressive radial stresses in the matrix are also greatly raised after the application of the stronger matrix (Fig. 12). At the inner radius of the matrix, the differences of the compressive radial stresses between the two different matrices are the largest. For the composites reinforced with the three types of fibers, the compressive radial stresses caused by the stronger matrix are about 11 times of those caused by the weaker matrix. When moving along the radial direction, they drop and become the externally applied tensile radial stress at the outer radius of the matrix. Once again, the radial stresses for the composites reinforced with radially and circumferentially orthotropic fibers are very close and bigger than those from a transversely isotropic fiber. Similarly, the tensile circumferential stresses in the matrix are greatly increased as well after introducing the stronger matrix (Fig. 13). At the inner radius of the matrix, the tensile circumferential stresses caused by the stronger matrix are about three times of those caused by the weaker matrix. Due to the same reason, the largest compressive radial stresses at the inner radius of the matrix result in the small tensile circumferential stresses at this position for both matrices according to Tresca's yield criterion. Then, along with the decrease of the compressive radial stresses, the tensile circumferential stresses increase and reach their maximum values at the interfaces between the elastic and plastic regions of the matrix. After that, they drop along with the increase of the radial coordinate. Compared to the increases of the radial and circumferential stresses at the inner radius of the matrix after the introduction of the stronger matrix, the increase of the axial stresses in the matrix is the smallest (Fig. 14). They are only raised by about 160% after employing the stronger matrix. Unlike the radial and circumferential stresses in the matrix which are very close for the composites reinforced with radially and circumferentially orthotropic fibers, such a closeness of the axial stresses is changed to the composites reinforced with circumferentially orthotropic and transversely isotropic fibers.

Since Matrix 2 is much stronger than Matrix 1, Matrix 2 has a bigger capacity to carry loads. Therefore, the plastic region of Matrix 2 is far smaller than that of Matrix 1. This can be seen from Fig. 15 where the elastic–plastic interfaces for the composites comprising Matrix 1 and the three types of fibers are at about $r = 55\,\mu m$, but they are changed to about $r = 45\,\mu m$ for the composites containing Matrix 2 and the same types of fibers. Like Matrix 1, in the region around the inner radius of the matrix, the stronger matrix also plastically yields. Tresca's equivalent stresses for the composites reinforced with the three types of fibers are the same and equal to the yield stress of Matrix 2. They keep unchanged until the matrix becomes elastic. Then, the matrix for the composites reinforced with a transversely isotropic fiber firstly leaves the plastic region resulting in a lower Tresca's equivalent stress than those from the composites reinforced with radially and circumferentially orthotropic fibers. Accompanying the further increase of the radial coordinate, all the Tresca's equivalent stresses go down and reach their minimum values at the outer radius of the matrix.

As pointed out by Avery and Herakovich [16] and indicated by Figs. 2, 3, 9 and 10, the circumferential and radial stresses at the center of radially orthotropic fibers are singular. For such fibers with Young's moduli and Poisson's ratios given in Table 1, λ_{f1} and λ_{f2} are less than unity. According to the first two of Eq. (22), the radial and circumferential stresses become singular at $r = 0$ since $\lambda_{f1} - 1$ and $\lambda_{f2} - 1$ are negative.

Conclusions

In this paper, an analytical approach has been developed to tackle the thermomechanical analysis of the composites consisting of anisotropic fibers and an elastic-perfectly plastic matrix. With the developed method, the deformations and stresses in the composites subjected to axisymmetric thermomechanical loads can be described with analytical formulae.

The effect of the elastic-perfectly plastic property of the matrix on the thermomechanical stresses in the composites reinforced with circumferentially orthotropic, radially orthotropic and transversely isotropic fibers is investigated. For the composite systems and the thermomechanical loads given in this paper, the elastic-perfectly

plastic property of the matrix reduces the compressive stresses in the fiber and the tensile circumferential and axial stresses in the matrix.

How different matrix materials affect the thermomechanical stresses in the composites has also been examined. By replacing a weaker matrix with a stronger matrix which has a higher thermal expansion coefficient, Young's modulus and Poisson's ratio, we found that the compressive stresses in the fiber and the tensile circumferential and axial stresses in the matrix are greatly increased. In addition, the plastic region of the matrix is obviously reduced. It indicates that a strong matrix can raise the load-carrying capacity of the composites. However, on the other hand, the increase of the stresses in the fiber raises the risk of the fiber failure.

References

1. Iesan D (1980) J Therm stress 3(4):495
2. Mikata Y, Taya M (1985) J Composite Mater 19:554
3. Arsenault RJ, Taya M (1987) Acta Metallurgica 35(3):651
4. Warwick CM, Clyne TW (1991) J Mater Sci 26:3817
5. Gardner SD, Pittman CU Jr, Hackett RM (1993) Compos Sci Technol 46(4):307
6. Gardner SD, Pittman CU Jr, Hackett RM (1993) J Compos Mater 27(8):830
7. Jayaraman K, Reifsnider KL (1992) J Compos Mater 26(6):770
8. Jayaraman K, Reifsnider KL (1993) Compos Sci Technol 47(2):119
9. Szyszkowski W, King J (1995) Comput Struct 56(2–3):345
10. Zhang H, Anderson PM, Daehn GS (1994) Metallurg Mater Trans A 25A:415
11. Choo H, Bourke MAM, Daymond MR (2001) Compos Sci Technol 61:1757
12. You LH, Long S (1998) Compos Part A 29A:1185
13. You LH, Long S, Rohr L (1999) J Appl Mech Trans Am Soc Mech Eng 66:750
14. Khan AS, Huang S (1995) Continuum theory of plasticity. John Wiley & Sons, Inc
15. You LH (2002) Compos Sci Technol 62:2209
16. Avery WB, Herakovich CT (1986) J Appl Mech Trans Am Soc Mech Eng 53:751
17. You LH (2002) Sci Eng Compos Mater 10(4):297
18. You LH (2002) Metallurg Mater Trans A 34A:883
19. Pindera M-P, Freed AD, Arnold SM (1993) Int J Solids Struct 30(9):1213